Elsevier Editorial System(tm) for Journal of Environmental Radioactivity

Manuscript Draft

Manuscript Number: JENVRAD-D-16-00138R1

Title: Applying multivariate statistics to discriminate uranium ore concentrate geolocations using (radio)chemical data in support of nuclear forensic investigations

Article Type: Research Paper

Keywords: Principal components analysis
nuclear forensics
radiochemical data
high-resolution gamma spectrometry
borate fusion

Corresponding Author: Mr. David George Reading, MSci

Corresponding Author's Institution: University of Southampton

First Author: David George Reading, MSci

Order of Authors: David George Reading, MSci; Ian W Croudace; Phillip E Warwick; Kassie A Cigliana

Abstract: The application of Principal Components Analysis (PCA) to U and Th series gamma spectrometry data provides a discriminatory tool to help determine the provenance for illicitly recovered uranium ore concentrates (UOCs). The PCA is built upon a database of radiometric signatures from 19 historic UOCs from Australia, Canada, and the USA representing many uranium geological deposits. Radiometric data are obtained via gamma and alpha spectrometry after the UOCs have been dissolved using lithium tetraborate fusion. Six UOCs from the same sample set were analysed 'blind' and compared against the database to identify their geolocation. These UOCs were all accurately linked to their correct geolocations which can aid the forensic laboratory in determining which further analytical techniques should be used to improve the confidence of the particular location.

Highlights

1. Principal Components Analysis is used as geolocating tool for nuclear forensics.
2.High quality radiometric signatures for uranium ore concentrates obtained using a rapid and effective dissolution technique.
3.”Unknown” samples are statistically compared against a database of known signatures.

Abstract

The application of Principal Components Analysis (PCA) to U and Th series gamma spectrometry data provides a discriminatory tool to help determine the provenance of illicitly recovered uranium ore concentrates (UOCs). The PCA is applied to a database of radiometric signatures from 19 historic UOCs from Australia, Canada, and the USA representing many uranium geological deposits. In this study a key process to obtain accurate radiometric data (gamma and alpha) is to digest the U-ores and UOCs using a lithium tetraborate fusion. Six UOCs from the same sample set were analysed 'blind' and compared against the database to identify their geolocation. These UOCs were all accurately linked to their correct geolocations which can aid the forensic laboratory in determining which further analytical techniques should be used to improve the confidence of the particular location.

1. Introduction

One of the main objectives of nuclear forensic science is to investigate and determine the geographical origin (or geolocation) of illicitly recovered nuclear materials via specific characteristics that are unique to that particular specimen. The necessity and demand for such investigations is amply demonstrated by the existence of IAEA's Incident and Trafficking Database (ITDB) where 257 cases of recovered or discovered nuclear material were reported in 2014 (IAEA, 2015). Due to the confidentiality and security of the ITDB in protecting IAEA member states' declarations, it is not known how many of these incidents directly involved uranium ore concentrates (UOC). However, a limited number of studies and media reports suggest that in the last decade, several large scale trafficking incidents of UOC have been intercepted including the seizure of 324 kg of UOC in Namibia (NTI, 2012a), the seizure of 170 kg stolen from Rossing Mine (Blake, 2011; NTI, 2012b) and the foiled attempt to sell and transfer 1000 metric tonnes of UOC to Iran (Mutua, 2015). The ability to confidently identify potential geolocations of such recovered samples rapidly and accurately is a key area of interest for nuclear forensic investigations.

This study explores the use of multivariate statistical analysis (Principal Components Analysis, PCA) using radiometric data obtained from uranium ore concentrates (UOC or "yellowcake"). Whilst PCA analysis has traditionally been applied to identify trends and groupings in data, it has rarely been employed as a discriminatory method where statistical comparisons are made between a database of signatures and the unknown to identify a single sample or family of samples (Ho Mer Lin et al., 2015; Keegan et al., 2008; Klunder et al., 2013; Lin et al., 2015; Robel et al., 2009; Švedkauskaitė-LeGore et al., 2008)

Gamma spectrometric data were selected as the investigative signature for the PCA as uranium ore milling causes radioactive disequilibrium in the uranium and thorium decay chains. Many of the associated radionuclides in these chains emit gamma photons on decay enabling observations on the extent of disequilibrium. The disequilibrium is due to the preferential leaching and precipitation of uranium from

the ore feed resulting in absent or very low concentrations of other uranium and thorium progeny radionuclides in the final UOC which could be diagnostic of a particular uranium mill. This gamma spectrometric signature consists of data from ^{234}Th, ^{234m}Pa, ^{214}Pb, ^{210}Pb, ^{235}U, ^{228}Ac and ^{208}Tl.

High-resolution gamma spectrometry (HRGS) is recommended by the nuclear forensics International Technical Working Group as one of the first experimental procedures that should be conducted on receipt of nuclear material for forensics investigations (Hanlen, 2011; Hutcheon et al., 2013; Kristo, 2012; Mayer et al., 2005; Wallenius et al., 2006, 2014). Therefore, the use of a statistical technique incorporating data from the first experimental procedure would enhance the investigation by providing the laboratory with an initial geolocation possibility. This information could guide the laboratory to narrow the field of geolocation options.

HRGS is typically used in non-destructive mode and serves to preserve the sample. It can often be applied with few problems when studying homogenised samples, such as uranium fuel pellets since photon detection efficiencies can be adjusted to reflect the uniform sample density. This relationship becomes more difficult to estimate when a sample has a heterogeneous matrix such as uranium ore and UOC which typically consist of higher density uranium-bearing minerals (typically between 5 and 8.5 g cm^{-3}) of variable grain size dispersed within lower density mineral phases (e.g. quartz, feldspars, micas, carbonates and iron-oxides; Figure 1).

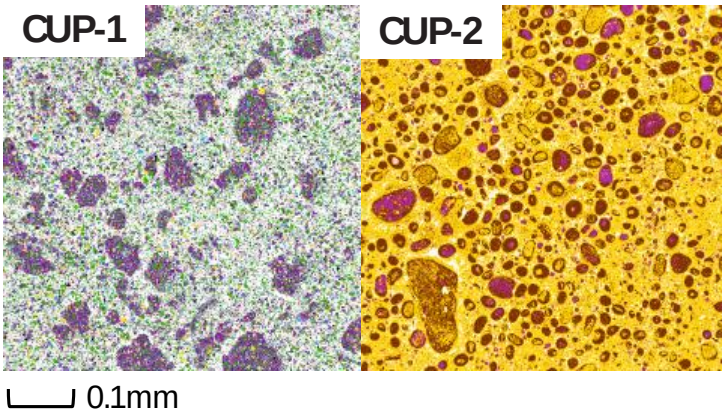

Figure 1. QEMSCAN false-colour images for CCRMP certified reference materials CUP-1 (U-ore) and CUP-2 (UOC). CUP-1 agglomerations (purple) are composed of muscovite and biotite mica with silicates. The gangue is composed of feldspars, pyrite, ankerite, apatite and calcite. CUP-2 agglomerations are composed of U-carbonates (pink and brown). The surrounding matrix (yellow) is composed of other U-phases.

The higher density grains in such heterogeneous matrices cause significant self-attenuation of low to medium energy (<200 keV) gamma photons (^{210}Pb, ^{234}Th, ^{226}Ra, ^{235}U) with minor but still significant effects on high energy gamma photon such as ^{234m}Pa (1001 keV) (Reading et al., 2015).

To accurately characterise U-ore and UOC via HRGS without the requirement for attenuation correction factors as used in environmental samples (Cutshall et al., 1983; Długosz-Lisiecka and Bem, 2013; Pilleyre et al., 2006; Sima and Dovlete, 1997), an effective and rapid preparative procedure was applied using a lithium tetraborate fusion that readily dissolves all components of the sample matrix (Croudace et al., 1998; Reading et al., 2015). The subsequent quenched glass is quickly dissolved in nitric acid resulting in a homogeneous, aqueous sample with significantly reduced self-attenuation effects with a density closer to aqueous calibration standards.

In this study a comparison between the pre- and post-dissolution gamma spectrometric data for a set of UOCs is made. This demonstrates the benefits of using lithium borate fusion to remove particle/density effects in UOCs and uranium

ores. The procedure enables trends and anomalies from the uranium ore feed and milling process to be identified which might otherwise would be missed in the traditional HRGS screening of illicitly recovered UOCs.

1.1 Uranium Ore Concentrates

A set of 19 UOCs were supplied by research partners at the Atomic Weapons Establishment (AWE) that represent part of a large, diverse and historical UK collection of samples originally derived from the former BNFL Springfields site (now managed and operated by Westinghouse Electric UK Ltd on the NDA's behalf). This valuable archive was catalogued, rationalised and made available to selected members of the international nuclear forensics community for R&D purposes. The names of the UOCs (derived from sources in Australia, Canada and the USA; Figure 2) are given based on the mine site, mill site, or the company responsible for the sample production. Therefore, some similarities could be observed between UOCs as mine/mill sites were sold between companies (for example Faraday and Madawaska – see table 1a and b). The ore feeds for each UOC are from a variety of localities and geological settings (Table 1a and Figure 2) and processing techniques (Table 1b).

113 **Table 1a: UOC localities, deposit types and mineralogy**

114

	Country of origin	Milling Facility	Uranium Deposit Type	Known Uranium Minerals	Other Minerals in Ore Feed
Anaconda	USA	Grants / Bluewater	SSt – Tabular	Coffinite, uraninite,	Calcite, chlorite, ferrosilite, marcasite, pyrite, quartz
Blind River	CAN	Elliot Lake	QPC	Brannerite, coffinite, uraninite	Apatite, cassiterite, garnet, Ilmenite, magnetite, pyrite (5-20%), rutile, titanite, zircon
Chevron Hill	USA	On-site	Sst – Roll front	Autunite, coffinite, uraninite,	Pyrite, marcasite
Cotter	USA	Canon City	Sst & vein (3:1)	Coffinite, Pitchblende	Ankerite, pyrite, quartz, minor Cu, Pb, Zn sulphides
Eldorado	CAN	On-site	Vein	Pitchblende, uraninite	Calcite, pyrite, quartz
Faraday[1]	CAN	On-site	Intrusive	Uraninite, uranophane, uranothorite	Amphibole, chalcopyrite, molybdenite, pyroxene, quartz, tourmaline
Gunnar	CAN	On-site	Vein	Pitchblende, uranophane	Chalcopyrite, chlorite, galena, kaolinite, pyrite, quartz
Lucky McGill	USA	On-site	Sst – Roll front	Coffinite, uraninite	Ferrosilite, jordisite, marcasite, pyrite, Mo, Se and V accessory minerals
Madawaska[1]	CAN	On-site	Intrusive	Uraninite, uranophane, uranothorite	Amphibole, chalcopyrite, molybdenite, pyroxene, quartz, tourmaline
Mary Kathleen	AUS	On-site	Metamorphic	Uraninite	Albite, allanite, epidote, garnet, K-Fels, REE minerals
Mesa EFI	USA	On-site	Collapse breccia pipe	Coffinite, torbenite, uraninite	Silicate minerals
			Sst	Carnotite	Vanadium minerals
Mulberry	USA	On-site	Phosphate	U recovered from phosphoric acid production	
North Span[2]	CAN	On-site / Elliot Lake	QPC	Brannerite, coffinite, uraninite, uranophane, uranothorite	Chlorite, monazite, pyrite, quartz, sericite
Olympic Dam	AUS	On-site	Haematite Breccia Complex	Brannerite, coffinite, pitchblende	Bornite, chalcocite, chalcopyrite, haematite, quartz, REE minerals
Queensland	AUS	On-site	UR	Autunite, brannerite, coffinite, torbenite, uraninite	Chlorite, Fe-oxides, sericite
Rabbit Lake	CAN	On-site	UR	Pitchblende, uranophane	Dickite, kaolinite, sulphides, vermiculite
Ranger	AUS	On-site	UR	Pitchblende, uraninite,	Chlorite, kaolinite, muscovite, quartz
Rio Algom[3]	CAN	Elliot Lake	QPC	Brannerite, coffinite, uraninite, uranophane, uranothorite	Chlorite, monazite, pyrite, quartz, sericite
South Alligator	AUS	Rockhole Creek	UR	Autunite, pitchblende, uraninite	Au, Pd and Pt minerals

Table 1b: UOC milling process

	Dissolution Process	Extraction Process for U	Precipitation process	Drying	References for Table 1a & b
Anaconda	Acid leach with MnO_2	SX-TA Chloride strip	MgO	Steamed	(IAEA, 1976)
Blind River	H_2SO_4 acid leach	Fixed bed ion exchange	NH_3	Calcined 800 °C	(Dahlkamp, 1993; IAEA, 1980)
Chevron Hill	Acid leach	SX	NH_3		(Albrethson, H., McGinley, 1982; IAEA, 1980)
Cotter	Carbonate leach with O_2	SX-TA $(NH_4)_2SO_4$ strip	NH_3		(IAEA, 1980, 1976)
Eldorado	Carbonate leach with O_2		NaOH	Steamed	(IAEA, 1980)
Faraday[1]	Acid leach with $NaClO_3$	IX NaCl strip	MgO		(IAEA, 1980; Proulx, 1997)
Gunnar					(IAEA, 1980)
Lucky McGill	Acid leach with $NaClO_3$	ELUEX	NH_3		(Albrethson, H., McGinley, 1982; IAEA, 1980)
Madawaska[1]	Acid leach with $NaClO_3$	IX NaCl strip	MgO		(IAEA, 1980; Proulx, 1997)
Mary Kathleen	Acid leach with MnO_2	SX-TA NH_3 strip	NH_3	Calcined	(Alfredson, 1980; IAEA, 2009, 1993, 1980)
Mesa EFI	H_2SO_4 acid leach with $NaClO_3$	SX-TA in kerosene NaCl strip	NH_3	Calcined at 590 °C	(IAEA, 1993, 1980)
Mulberry	U recovered from phosphoric acid production				
North Span[2]					(IAEA, 1976)
Olympic Dam	Acid leach with $NaClO_3$	SX-TA in kerosene	NH_3	Calcined at 750 °C	(Dahlkamp, 1993; Edwards and Oliver, 2000; IAEA, 2009, 1993, 1980)
Queensland	Acid leach with MnO_2	SX-TA NH_3 strip	NH_3	Calcined	(Alfredson, 1980; IAEA, 1980)
Rabbit Lake	Acid leach with $NaClO_3$	SX-TA $(NH_4)_2SO_4$ strip	NH_3	Calcined 650 °C	(Edwards and Oliver, 2000; IAEA, 1993)
Ranger	Acid leach with MnO_2	SX-TA $(NH_4)_2SO_4$ strip	NH_3	Calcined	(IAEA, 1980)
Rio Algom[3]	H_2SO_4 acid leach with O_2.	IX H_2SO_4 strip	MgO & $CaCO_3$ or CaO & NH_3		(IAEA, 1993, 1980)
South Alligator	H_2SO_4 acid leach.	SX with NaCl	MgO		(Alfredson, 1980; IAEA, 2009)

[1] Faraday and Madawaska are the same mine sites. Faraday operated 1954-1964 and Madawaska operated 1975-1982.

[2] North Span (company) operated many mines that Rio Algom (company) then purchased. Mineralogy for North Span inferred from Rio Algom records.

[3] Rio Algom operated many mines of which Panel, Stanleigh and Quirke mines are the most likely source for this sample.

QPC = Quartz-pebble conglomerate; Sst = Sandstone; UR = Unconformity related

SX–TA = Solvent exchange with tertiary amine; IX = Ion exchange; ELUEX = Eluate Extraction - H_2SO_4 leach with amine extraction in a joint application.

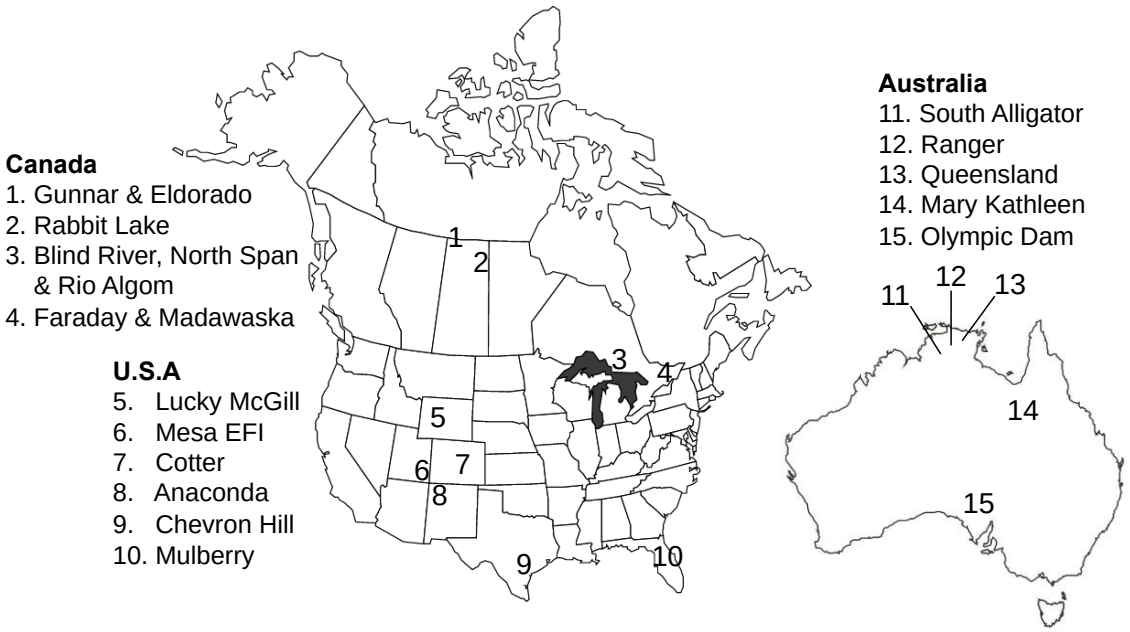

Figure 2: Geographical locations of U mines and milling facilities used to manufacture the UOCs in this study.

2. Methodology

2.1 Instrumentation

Gamma emitting radionuclide activity concentrations were determined using Canberra 50% N-type HPGe well-type spectrometers. The spectra were collected using Genie 2000 acquisition software (Canberra Industries, Harwell, UK) and were analysed using Fitzpeaks spectral deconvolving software (JF-Computing, Stanford in the Vale, UK). The spectrometers were calibrated using spiked radionuclide standards throughout several "density geometries" (matrices of cellulose, water, sand, steel and boron, and a tin-tungsten ore). A mixed nuclide source (NPL, Teddington, UK) and a ^{210}Pb solution standard (PTB, Braunshweig, Germany) were used. All samples were counted for 1 h as low detection limits and low counting uncertainty (< 6% relative ^{234}Th fused matrix and < 16% relative ^{234}Th solid matrix) were achievable with this count time.

The ^{210}Pb activity concentrations were determined via the alpha emitting grand-daughter radionuclide ^{210}Po, that had been plated onto silver discs (Flynn, 1968) and counted using an Ortec PC alpha spectrometer system fitted with 450 mm^2 Ultra

detectors. All measurements were made *in vacuo* for 36 hours. Spectra were acquired using Maestro 7 and analysed by WinPlots 7 (AMETEK, Wokingham, UK).

2.2 Initial characterisation of UOCs

Approximately 10 g of each UOC was weighed into 20 mL polythene vials and sealed for at least 21 days using Viton rubber discs to prevent loss of radon and to establish secular equilibrium between ^{226}Ra, ^{222}Rn and ^{214}Pb. The photon efficiency for each measured radionuclide from the UOCs was calculated based on the bulk density of the sample and the known relationship between sample density and photon efficiency acquired from the calibration standards. The samples were characterised for ^{234}Th, ^{234m}Pa, ^{214}Pb, ^{210}Pb, ^{235}U, ^{228}Ac and ^{208}Tl where ^{234}Th and ^{234m}Pa is measured as a proxy for the non-gamma-emitting ^{238}U; ^{214}Pb (a proxy for ^{226}Ra) and ^{210}Pb was measured to assess the efficiency of the uranium milling, processing and/or contamination; and ^{228}Ac and ^{208}Tl are measured as proxies for ^{232}Th.

2.3 Borate fusion for homogenisation

Sub-samples of UOC were blended at a 1:1 ratio with di-lithium tetraborate flux (Fluxana, Germany) and fused to ~1100 °C with periodic agitation for 5 minutes. The resulting melt was quenched by pouring the melt into a beaker containing 50 mL Milli-Q water (Millipore, USA). After all the glass fragments had settled the excess water was carefully decanted and 8M analytical grade nitric acid (8 M) was then added to digest the sample at 50 °C using a PTFE stirring/hot-plate system. After digestion, any insoluble silica and boric acid (neither of which retained any activity) were removed by vacuum filtration. The sample was heated at 90 °C to reduce the sample volume to ~ 15 mL where it is then transferred to a glass scintillation vial fitted with a Viton rubber disc to retain ^{222}Rn, topped up to 20 mL with Milli-Q water and measured immediately. A more detailed methodology and rationale for this procedure can be found in Reading et al., (2015). During the fusion process, ^{222}Rn undergoes degassing and thus causes disequilibrium in activity concentration for the short-lived daughter radionuclides. Therefore, as previously mentioned, the samples

were sealed using a Viton disc and re-counted after 21 days. No other gamma emitting radionuclides demonstrate volatilisation using this procedure.

During any ore processing ^{226}Ra progeny are invariably lost. Monitoring for ^{226}Ra was performed but its low concentration and its single, low yield (3.6%) gamma emission and its interference from ^{235}U made direct measurement difficult. Instead, ^{214}Pb measurements were collected as a proxy for ^{226}Ra once secular equilibrium had been established after 21 days.

2.4 Preparation and measurement of ^{210}Po in UOC via autodeposition.

An aliquot of 150 µL (~ 3-4 mg UOC) of each fused solution was evaporated to dryness, spiked with ^{209}Po (0.275 Bq g^{-1}) as a yield monitor and dried again. The residue was digested with 8 ml of 6M HCl with the addition of 50 ml of Milli-Q Water and ~ 1 g ascorbic acid to prevent any iron present from plating on to a silver planchet (Benoit and Hemond, 1988; Lee et al., 2014). The planchet was covered on one side with PVC tape to limit autodeposition to one side. The planchet was supported by a plastic holder and positioned in the solution, which was covered for 48 hours at 25-30 °C for autodeposition. After this time, the planchet was removed, rinsed, and dried on a warm hotplate at 30 °C. The planchets were measured for 36-48 hours dependent on achieving a ^{209}Po peak area of at least 2000 counts.

The measured ^{210}Po (138.4 d) was decay corrected to the autodeposition completion date as ^{210}Pb is not co-deposited with the ^{210}Po. As ^{210}Po is lost during fusion, the measured ^{210}Po originates solely from ingrowth from ^{210}Pb since fusion. The measured ^{210}Po can therefore be used to determine the original ^{210}Pb activity in the sample. This is achieved by the utilisation of Bateman equations (equation 1) to calculate the initial ^{210}Pb activity concentration based on the decay corrected ^{210}Po activity concentration (A) and the known decay constants of ^{210}Pb (λ_1), ^{210}Bi (λ_2) and ^{210}Po (λ_3) over a period of time ($t = 123\ d$) where ingrowth has occurred. The decay and ingrowth calculation allow for accurate ^{210}Po (and therefore ^{210}Pb) activity concentration to be determined for each UOC.

$$^{210}Pb = \frac{A \,/\, \lambda 1 \,/\, \lambda 2}{\left(e\frac{-\lambda 1\, t}{(\lambda 2-\lambda 1)(\lambda 3-\lambda 1)}\right)+\left(e\frac{-\lambda 2\, t}{(\lambda 1-\lambda 2)(\lambda 3-\lambda 2)}\right)+\left(e\frac{-\lambda 3\, t}{(\lambda 1-\lambda 3)(\lambda 2-\lambda 3)}\right)}$$

Equation 1.

2.5 Principal Components Analysis

Principal Components Analysis was selected as the statistical method of choice as it is a dimensionality reduction technique, whereby the least number of variable combinations, loading on to each component, are determined in order to explain the maximum amount of variance among the UOCs (Jolliffe, 2014; Tabachnick and Fidell, 2013). PCA was selected over other multivariate techniques such as factor analysis, which typically accounts for both variance and covariance (Brown, 2006), due to the nature of the dataset. The variables (radionuclides) in each UOC occur naturally together; therefore they will always correlate strongly so the covariance of the radionuclides does not need to be an area of focus. This study therefore relies on PCA's ability to focus on variance among the samples, which will maximise its potential as a discriminatory technique. Equally, other classification techniques, such as cluster analysis, must be discounted because of the relatively low number of radionuclides measured in the data and the reoccurrence of certain radionuclides across more than one of the significant components.

The PCA in this study was completed using SPSS 21 (IBM). This technique groups related dependent variables (in this case the radionuclides) into a series of components by calculating an eigenvalue for each group of variables (Jolliffe, 2014; Smith, 2002). An eigenvalue is a linear representation of the amount of variance explained by the grouping of dependent variables which load onto each component. Components may also contain differing numbers of dependent variables subject to the variance explained by each set. Variable groupings with higher eigenvalues will inevitably explain more variance among the samples than groupings with a lower eigenvalue. A data set may contain an infinite number of components which could

be used to either group or distinguish the samples, however, for the purposes of the present PCA, only the three components with the highest eigenvalues are selected.

Each UOC in the data set is then assigned 3 component scores (CS) which were calculated based on each of the three components identified as having the highest eigenvalues. The CS for each UOC represent the quantity of each sample's radionuclide activity loaded onto each component, relative to the other samples and the mean value of each radionuclide. These CS values are essentially coordinates (x, y, z) which are used to plot each sample's radiometric properties in three-dimensional space. An Oblimin rotation was applied to the CS in order to visually represent the data in the clearest possible way in three-dimensions.

3. Results & Discussion

3.1 UOC activity concentration comparison between matrices.

The activity concentration discrepancy between the solid and fused gamma spectrometric measurements is proportional to the energy of the gamma emission associated with each radionuclide (Figure 3). This bias is most pronounced with ^{234}Th due to its low energy emissions where the mean measurements from the solid matrix are ~15% that of the fused measurements. Comparatively, the matrix bias for medium energy ^{235}U is 33% and the high-energy ^{234m}Pa is 88% although some samples are within uncertainty of one another. The solid and fused activity concentration discrepancy between ^{214}Pb, ^{228}Ac and ^{208}Tl is between 60-70%. These discrepancies are a result of photon attenuation within the complex, heterogeneous matrix despite photon detection efficiency adjustments for individual photon energies derived from sample bulk density. The cause, effects and difficulty in applying attenuation corrections to such sample matrices are discussed elsewhere (Reading et al. 2015).

The variation of U grain/agglomeration size and concentration between the UOCs explains why different patterns can be observed between the solid and fused

matrices in Figure 3; e.g. Lucky McGill – USA demonstrates the highest discrepancy for ^{234}Th, ^{235}U and ^{234m}Pa as it most likely contains the largest uranium grains or agglomerations and *vice versa* for Cotter – USA.

A discrepancy is observed between the two matrices for ^{214}Pb activity concentrations where the bias is proportional to the total ^{214}Pb present. The UOCs typically have < 10 Bq g^{-1} of ^{214}Pb with exception to Cotter – USA with ^{214}Pb activity of 28 ± 3 Bq g^{-1}. Five of the UOCs are below the lower limit of detection (LLD) of 0.7 Bq g^{-1}. The presence of ^{214}Pb is an indicator of the combined inefficiency of uranium ore milling and the ingrowth of ^{234}U daughter radionuclides. These data cannot be used as a chronometer for the UOC processing date, as an assumption would have to be made that the milling was 100% efficient at removing daughters of ^{234}U.

Actinium-228 and ^{208}Tl were detected in all of the Canadian UOCs with the exception of Rabbit Lake and were also detected in Cotter – USA indicating that these UOCs, despite undergoing uranium purification, have retained trace amounts of thorium minerals present from the ore feed. The thorium present equates to between 0.02 ± 0.01 wt% Th (Gunnar and Cotter) and 1.10 ± 0.1 wt% Th (Madawaska). The difference in activity concentration between ^{228}Ac and ^{208}Tl is due to the branching of ^{208}Tl (36%) and ^{212}Po (64%) from ^{212}Bi.

Activity concentrations for ^{210}Pb (46.6 keV) were not resolvable due to the Compton background and the large peak tailing from the nearby ^{234}Th photon peak energy of 63.3 keV resulting in a ^{210}Pb lower limit of detection of < 15 Bq g^{-1}. However, one sample (Cotter – USA) did have a measurable amount of ^{210}Pb (28.5 ± 2.3 Bq g^{-1}) within the fused matrix. The UOCs were measured using a Low Energy Germanium (LEGe) detector as its lower Compton background and improved resolution for low to medium energy photons, compared to HPGe, helped resolve the ^{210}Pb from the Compton background. As before, only Cotter-USA had resolvable ^{210}Pb and the remaining samples were all below the LLD (<10 Bq g^{-1}).

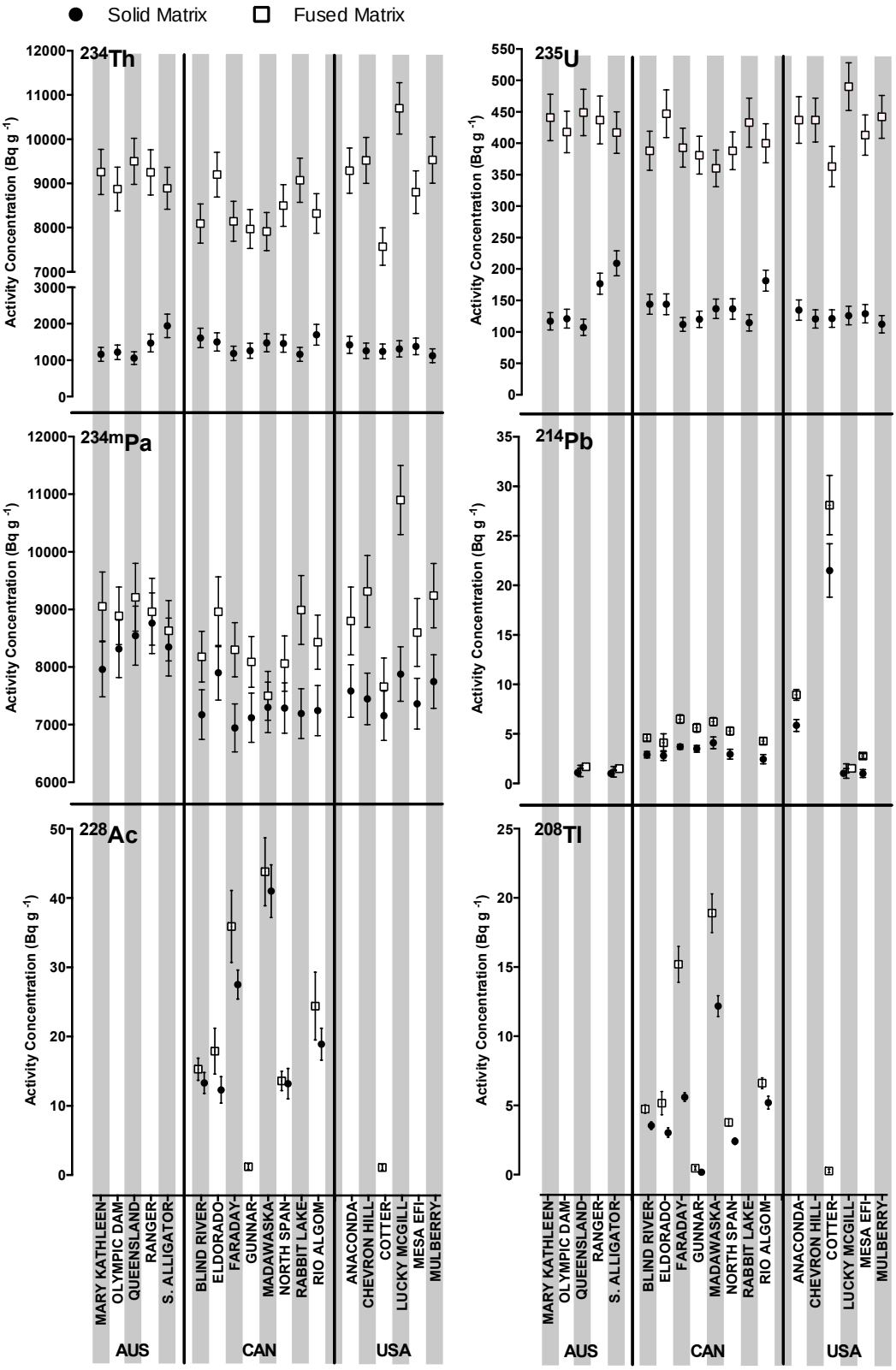

299 *Figure 3: Measured activity concentrations for ^{234}Th, ^{235}U, ^{234m}Pa, ^{214}Pb, ^{228}Ac and ^{208}Tl from*
300 *particulate and fused UOC sample matrices. LLD ^{214}Pb = < 0.7 Bq g^{-1}, LLD ^{228}Ac = < 0.2 Bq*
301 *g^{-1}, LLD ^{208}Tl = < 0.1 Bq g^{-1}. Uncertainty = 2σ.*

3.2 ^{226}Ra and ^{210}Pb activity concentrations and their ratio.

As ^{214}Pb activity concentrations were measurable in most of the UOCs via HRGS, it is reasonable to assume that ^{210}Pb would also be present due to the short half-lives of ^{214}Bi (26.8 m) and ^{214}Po (0.16 s). Due to the high LLD for ^{210}Pb as previously discussed, the grand-daughter radionuclide ^{210}Po was measured as a proxy using alpha spectrometry.

All of the UOCs had detectable amounts of ^{210}Po with the exception of Mulberry (Figure 4) where the ^{210}Po LLD = < 0.06 Bq g^{-1} (which is equivalent to ^{210}Pb LLD = 0.14 Bq g^{-1} with 123 d ingrowth). These data were then decay and ingrowth corrected to provide ^{210}Pb activity concentrations. Where available, the activity concentrations of ^{226}Ra (^{214}Pb) and ^{210}Pb (^{210}Po) for all but one sample results in an activity ratio of 1:1 (within uncertainty) demonstrating that there is no discernible disequilibrium between ^{226}Ra and ^{210}Pb. The North Span UOC does not have this characteristic due to the ^{210}Pb activity concentration being three-times greater than ^{226}Ra (Figure 4). The milling and processing of the North Span UOC may have been less efficient at removing ^{210}Pb from the uranium series decay products compared to ^{226}Ra or the sample may have become anthropogenically contaminated after processing. Nevertheless, this unusual characteristic could be a useful diagnostic feature for identifying this particular UOC sample for future identification purposes.

The preparation and measurement of ^{210}Po can be made immediately after fusion as ^{210}Pb is not affected by the procedure and therefore can act as a suitable proxy radionuclide for ^{226}Ra and its immediate daughters. A selection of UOCs was treated using acid digest to ensure retention of volatile ^{210}Po and to demonstrate the validity of the ingrowth and decay corrections for the fused samples. The two digestion approaches (i.e. acid and fusion) produced ^{210}Po activity concentrations that were in agreement within uncertainty.

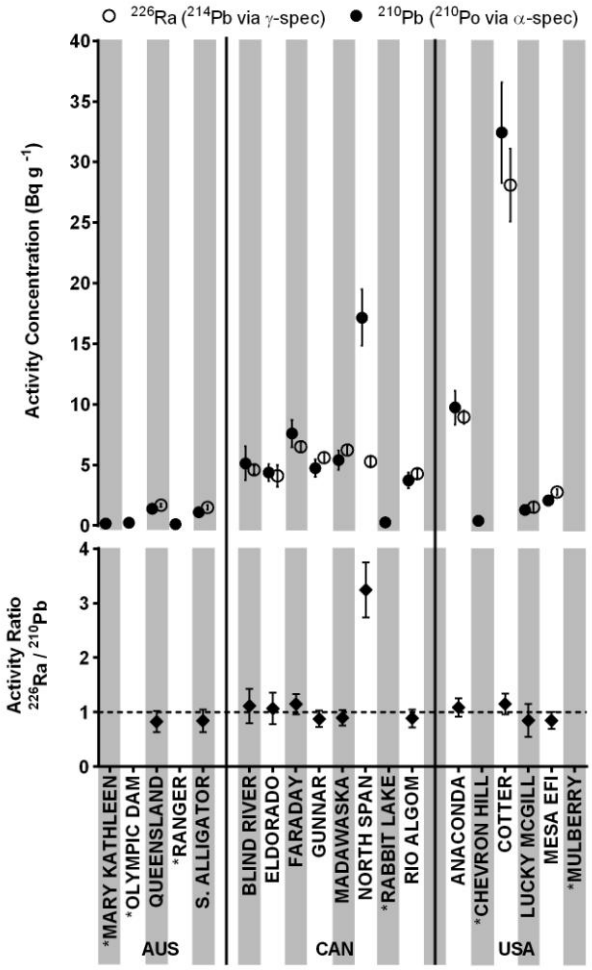

*Figure 4: ^{210}Pb (^{210}Po) and ^{226}Ra (^{214}Pb) activity concentration comparisons (top) and their associated ratio (bottom). * denotes where ratio is not available due to ^{226}Ra (^{214}Pb) activity concentration being below the LLD. Uncertainty = 2σ.*

3.3 Principal Components Analysis

The components for the PCA were selected in order to explain the maximum amount of variance possible among the UOCs' radionuclide activity concentrations whilst limiting the analysis to only three components (table 2). Lead-214 was removed from the PCA due to the incomplete data which would lower the percentage of variance of each component that it was originally assigned to.

Table 2. Components and associated variables used in the PCA

Component	Variable Selected	Eigenvalue	% of Variance *(cumulative)*
1	^{234}Th, ^{234m}Pa, ^{235}U, ^{228}Ac, ^{208}Tl, ^{210}Pb	4.05	67.46
2	^{228}Ac, ^{208}Tl, ^{210}Pb	1.37	22.80 *(90.26)*
3	^{210}Pb	0.49	8.20 *(98.46)*

In the first component, all of the radionuclides are included in the eigenvalue calculation; when analysed as a whole, the inter-relationships of these variables explain 67% of the total variance among the samples. However, as the PCA in this instance is being used as a discriminatory technique, the second and third components include only those radionuclides which vary most significantly from the wider group. Component two includes ^{228}Ac, ^{210}Pb and ^{208}Tl, which as a group varies most significantly from the wider grouping of radionuclides. The final component contains only ^{210}Pb due to its high variability among these UOCs. Together, the three components account for 98% of the total variance among the UOCs. The component scores for each UOC and thus their position in three-dimensional space are displayed in Figure 5. If the average activity concentration for all radionuclides from all the UOCs was plotted on the PCA in Figure 5, the coordinates would be $x = 0$, $y = 0$, $z = 0$.

The results of the PCA reveal a central cluster of UOCs, surrounded by a number of outlying samples across all three dimensions shown. Within the cluster, nine of the UOCs share similar CS2 and CS3 values, indicating very little variability among the ^{232}Th daughters and ^{210}Pb concentration. Conversely, the outlying UOCs demonstrate a much greater variability in their CS coordinates, indicating major fluctuation of the measured radionuclide concentrations in one or more of the component scores.

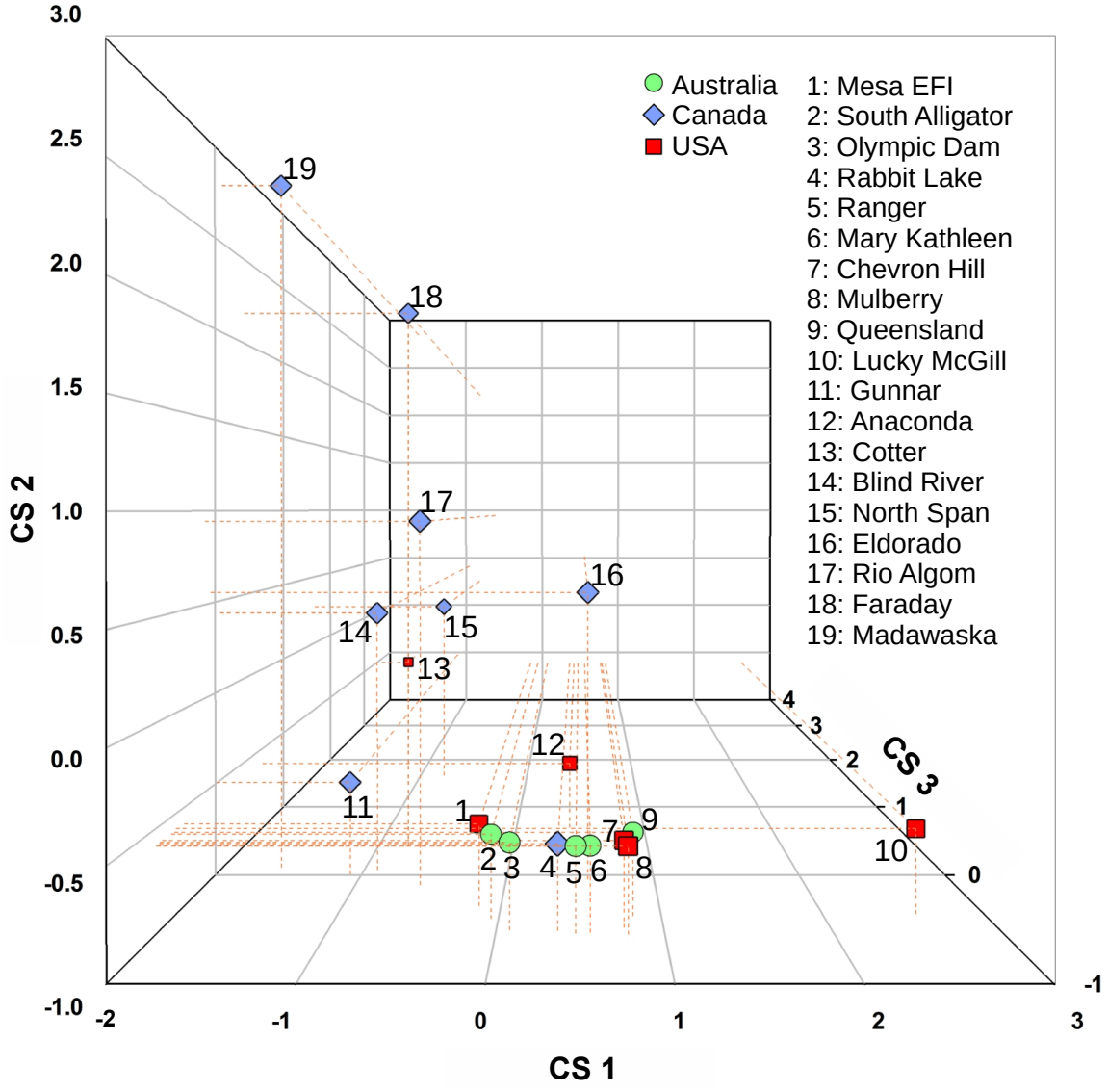

Figure 5: Three-dimensional Principal Components Analysis results using 3 components with associated component scores (CS) for each UOC.

Although this study only considers a limited number of UOC samples, it is clear that certain trends can be deduced. The Australian UOCs have all clustered in the central group meaning that the samples are all similar radiometrically and in terms of milling efficiency, regardless of the different mill locations and the mineralogy of the ore feed. The Canadian UOCs generally have a lower CS1 value than the central cluster, have highly variable CS2 values and have similar CS3 values to the central cluster with exception to North Span (point 15). The American UOCs generally have a similar CS1 score compared to the central cluster but have two UOCs that are

significantly higher (Lucky McGill - point 10) and lower (Cotter – point 13) than this group. The CS2 values are generally low among the American samples and do not show as much variance as the Canadian UOCs. The CS3 value is again similar to the central cluster but two of the samples have higher values (Anaconda – point 12 and Cotter – point 13).

Regardless of the UOCs geological origin, no trends could be observed between the type of geological deposit and the sample position within the PCA. Similarly, the known mineralogy of the local geology for each ore feed cannot be used to determine the provenance of a UOC. All but two of the Canadian samples exhibit elevated natural thorium activity concentrations suggesting that thorium-bearing minerals are present in these samples (PCA points 14-19) but ore feeds for PCA points 14 (Blind River) and 16 (Eldorado) are not known to contain elevated thorium concentrations. This could be an artefact of mixed ore feeds from various sites around the region so is not diagnostic of the mine site, but instead of the milling site. Similarly, four of the UOCs from the USA (Anaconda, Cotter, Lucky McGill and Mesa EFI) are from a region known for elevated thorium-bearing minerals and yet this is not evident in the PCA. Again, this is not necessarily an indicator of the mine site, but instead of the processing and milling site.

Despite the lack of significant differences in deposit type, mineralogy and known country of origin, the potential of the PCA as a discriminatory tool remains valid.

Although it would be difficult to match an unknown sample to a possible origin if it were to plot in the central cluster, it would allow, with statistical certainty, the laboratory to deduce that the unknown is not similar to any of the outlying positions thus reducing the possibilities of sample origin and *vice versa*. Though the PCA may not be able to indicate the likely origin all potential unknown samples, it could be used to mathematically determine the next best discriminatory technique(s) to deconvolve a group of unknowns based on the HRGS and alpha spectrometric data.

The PCA is unable to incorporate the uncertainty associated with each radionuclide when calculating the component scores associated for each sample as only the mean value is used. This is evident with the Faraday and Madawaska UOCs which are from the same, thorium-rich ore body and mill, where the Faraday site was operated between 1954-1964 and the Madawaska site was operated between 1975-1982 (IAEA, 1980; Proulx, 1997). The two UOCs demonstrate high CS2 values, little variance in CS3 and low CS1 values with respect to the central cluster. The minor difference in CS3 values would indicate that the milling efficiencies are near identical which is to be expected if the same mill and procedure is being used. The changes observed for CS1 and CS2 however, indicate that the second operational period as Madawaska had a lower U concentration and higher natural thorium concentration indicating a potential change in the ore feed. This may or may not be the case as scrutinising the data from Figure 1 would indicate that the two samples have the same uranium and thorium concentration within uncertainty. The two positions of Faraday and Madawaska on the PCA in an ideal situation would be closer together. Despite this, the two samples are significantly different from all of the other UOCs present in the PCA which demonstrates that the samples are most likely not related to any of the other UOCs.

Traditional exploratory statistical techniques such as correlations and analyses of variance (ANOVA) were also considered, but were unable to account for such a complex data set. These methods act by separating only two selected variables for analysis, whilst inter-relationships among the larger set of dependent variables typically cannot be accounted for within complex data sets. Thus, the analysis of such inter-relationships using PCA might be better able to discriminate one UOC from another more so than correlations and ANOVA alone due to its organisation of inter-related variables into a number of components.

3.4 Experimental and Statistical Validation

The robustness and reproducibility of the experimental procedure and statistical approach was validated by re-preparing and re-counting six UOCs, two from each

country which demonstrated the most variance based on the original PCA in an attempt to identify whether a large database containing UOC radiological data could be used as a discriminatory and provenance determining tool. The six UOCs were: Cotter, Eldorado, Faraday, Lucky McGill, Queensland and South Alligator. The radiometric data of the six “unknown” samples was added to the pre-existing PCA database and the results are shown in Figure 6.

The six “unknown” samples plot close to their original positions as determined in the original PCA indicating that the experimental procedure and statistical approach can be replicated and therefore can be used as a discriminatory tool. Additionally, it demonstrates that not incorporating measurement uncertainty in the component score calculation is not detrimental to the overall analysis in determining where an “unknown” samples plots among previously characterised samples.

For the Canadian and American UOCs, the “unknown” UOCs plot next to the original PCA data indicating that with high amount of certainty, these UOCs can only come from one potential origin. This becomes more complicated for the Australian UOCs where so many UOCs are positioned in close proximity in the central cluster. In this instance, it is unadvisable to attempt to identify an exact origin for the UOC but instead to eliminate which UOCs the “unknown” sample cannot be.

With such a small UOC dataset, it is relatively simple to discriminate between the 19 samples. This will inevitably become more complicated if a larger UOC radiological database was created representing historic and current UOC production. However, as demonstrated with the Australian UOCs, if an “unknown” sample cannot be attributed to a single provenance, it can at least reduce the number of suspected origins greatly. Similarly, if an “unknown” sample plots near a group of UOCs that are known to have highly variable rare earth element (REE) signatures, the laboratory may decide that an investigation in to REE signatures is the best discriminatory method to apply to further discriminate the samples.

The composition of an ore feed will vary over time depending on whether multiple mine sites are being processed simultaneously at one mill, or whether significant intra-mine compositional variability is possible from large deposits. Regardless, the processing technique, parameters and purification efficiency for UOC production will remain constant for extended periods time. This results in consistent uranium grade and levels of impurities (daughter radionuclides) and is diagnostic of the mill during a particular period of operation.

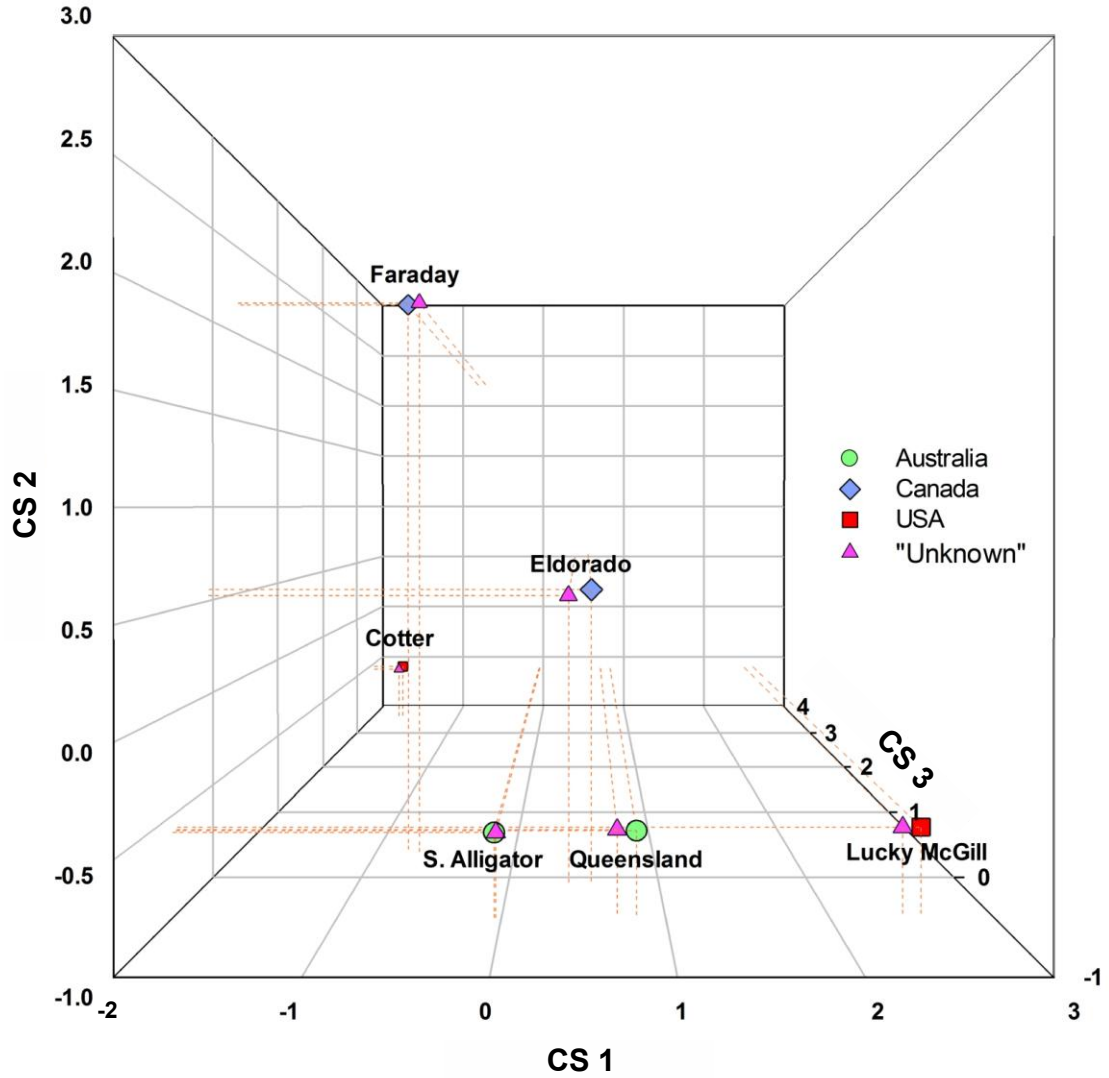

Figure 6: Three-dimensional Principal Components Analysis results for experimental and statistical validation of techniques. CS = component score.

4. Conclusion

This study has shown that Principal Component Analysis PCA is a useful nuclear forensic tool that can help indicate the origin of unknown, illicitly recovered UOCs. The study used 19 UOC samples to build a database of radiometric signatures based on gamma and alpha spectrometry.

Prior to any applications using gamma spectrometry data it is critical that matrix and absorption effects are adequately compensated for otherwise data accuracy will be diminished. Variable density samples such as U ores and UOCs are particularly susceptible to matrix/particle problems especially significant for radionuclides having only low energy gamma energies. The elimination or reduction of matrix and particle effects can be effectively dealt with using specific digestion methods and in this study a borate fusion is shown to ensure rapid dissolution and accurate data.

The results from the PCA demonstrate that some UOCs group together due to their similar radiometric properties, whereas over 50% of the samples are outliers and are statistically different from one another. Six of these UOCs were re-prepared, measured and scrutinised via PCA in an attempt to validate the experimental and statistical approaches. The “unknown” samples plotted consistently close to their original data points showing that such an experimental and statistical approach can be used for matching an “unknown” sample against known samples within a database for determining the origin of UOCs.

Where an unknown sample plots near a cluster of radiometrically similar samples, the laboratory may be in a better position to determine the next analytical technique required to further constrain the origins of the unknown based on a signature which is known to be different amongst the particular cluster of samples.

For such a technique to be applied for current and future nuclear forensic investigations on illicitly recovered specimens, UOCs representing historic and currently operating uranium mills would need to be profiled for their radiometric

properties in order to potentially match a recovered sample in the future. Extending the number of characterised UOCs in this database is strongly recommended.

5. Acknowledgements

The authors thank the AWE Outreach Programme (AWE 30200056) for funding this PhD project (for DGR).

6. References

Albrethson, H., McGinley, F.E., 1982. Summary History of Domestic Uranium Procurement Under U.S. Atomic Energy Commision Contracts Final Report.

Alfredson, P.G., 1980. Australian experience in the production of yellow cake and uranium fluorides, in: Production of Yellow Cake and Uranium Fluorides. IAEA, Vienna, pp. 149–178.

Benoit, G., Hemond, H.F., 1988. Improved methods for the measurement of ^{210}Po, ^{210}Pb, and ^{226}Ra. Limnol. Oceanogr. 33, 1618–1622.

Blake, H., 2011. Wikileaks: uranium bricks and radioactive trains among nuclear terror scares. The Telegraph, London (02/02/2011).

Brown, T.A., 2006. Confirmatory factor analysis for applied research, 2nd ed. Guilford Press, New York, USA.

Croudace, I., Warwick, P., Taylor, R., Dee, S., 1998. Rapid procedure for plutonium and uranium determination in soils using a borate fusion followed by ion-exchange and extraction chromatography. Anal. Chim. Acta 371, 217–225.

Cutshall, N.H., Larsen, I.L., Olsen, C.R., 1983. Direct Analysis of ^{210}Pb in Sediment Samples: Self-Absorption Corrections. Nucl. Instruments Methods 309–312.

Dahlkamp, F., 1993. Uranium Ore Deposits. Springer, Berlin, Germany.

Długosz-Lisiecka, M., Bem, H., 2013. Fast procedure for self-absorption correction for low γ energy radionuclide ^{210}Pb determination in solid environmental samples. J. Radioanal. Nucl. Chem. 298, 495–499.

Edwards, C.R., Oliver, A.J., 2000. Uranium processing: A review of current methods and technology. J. Miner. Met. Mater. Soc. 52, 12–20.

Flynn, W.W., 1968. The determination of low levels of polonium-210 in environmental materials. Anal. Chim. Acta 43, 221–227.

Hanlen, R., 2011. Round Robin 3 Exercise After Action and Lessons Learned Report. PNNL-20079. Pacific Northwest Natl. Lab. U.S. Dep. Energy, Richland, WA.

Ho Mer Lin, D., Jones, A.E., Goulermas, J.Y., Turner, P., Varga, Z., Fongaro, L., Fanghänel, T., Mayer, K., 2015. Raman spectroscopy of uranium compounds and the use of multivariate analysis for visualization and classification. Forensic Sci. Int. 251, 61–68.

Hutcheon, I.D., Kristo, M.J., Knight, K.B., 2013. Nonproliferation Nuclear Forensics, in: Uranium - Cradle to Grave. Winnipeg, pp. 377–394.

IAEA, 2015. IAEA Incident and Trafficking Database (ITDB). Vienna, Austria.

IAEA, 2009. World Distribution of Uranium Deposits (UDEPO) with Uranium Deposit Classification 2009 (TECDOC-1629). Vienna, Austria.

IAEA, 1993. Uranium Extraction Technology (Technical Report Series No. 359). Vienna, Austria.

IAEA, 1980. Significance of Mineralogy in the Development of Flowsheets for Processing Uranium Ores (Technical Reports Series No. 196). Vienna.

IAEA, 1976. Uranium Ore Processing, in: Proceedings of an Advisory Group Meeting Washington, DC. Vienna.

Jolliffe, I., 2014. Principal Component Analysis, in: Wiley StatsRef: Statistics Reference Online.

Keegan, E., Richter, S., Kelly, I., Wong, H., Gadd, P., Kuehn, H., Alonso-Munoz, A., 2008. The provenance of Australian uranium ore concentrates by elemental and isotopic analysis. Appl. Geochemistry 23, 765–777.

Klunder, G.L., Plaue, J.W., Spackman, P.E., Grant, P.M., Lindvall, R.E., Hutcheon, I.D., 2013. Application of visible/near-infrared reflectance spectroscopy to uranium ore concentrates for nuclear forensic analysis and attribution. Appl. Spectrosc. 67, 1049–1056.

Kristo, M.J., 2012. Handbook of Radioactivity Analysis, Third edit. ed. Elsevier, San Diego.

Lee, H.M., Hong, G.H., Baskaran, M., Kim, S.H., Kim, Y.I.L.L., 2014. Evaluation of plating conditions for the recovery of ^{210}Po on a Ag planchet. Appl. Radiat. Isot. 90, 170–176.

Lin, M., Zhao, Y., Zhao, L., Li, L., Wang, F., Zhu, L., Hu, X., Ning, W., 2015. Tracing origins of uranium ore concentrates (UOCs) by multidimensional statistical analysis of rare-earth impurities. J. Anal. At. Spectrom. 30, 396–402.

Mayer, K., Wallenius, M., Ray, I., 2005. Nuclear forensics - a methodology providing clues on the origin of illicitly trafficked nuclear materials. Analyst 130, 433–41.

Mutua, J.-M., 2015. Uranium yellowcake trafficking incidents in Africa. African Secur. Rev. 24, 162–189.

NTI, 2012a. 2011 Illicit Trafficking Incidents [WWW Document]. Nucl. Threat Initiat. URL: http://www.nti.org/media/pdfs/2011_illicit_trafficking_incidents_2.pdf?_=1370293383 (accessed 27/04/2016).

NTI, 2012b. Namibia: 170 kg of natural uranium stolen from Rossing Mine [WWW Document]. URL: http://www.nti.org/analysis/articles/namibia-170-kg-natural-uranium-stolen-rossing-mine/ (accessed 27/04/2016).

Pilleyre, T., Sanzelle, S., Miallier, D., Faïn, J., Courtine, F., 2006. Theoretical and experimental estimation of self-attenuation corrections in determination of ^{210}Pb by gamma spectrometry with well Ge detector. Radiat. Meas. 41, 323–329.

Proulx, M., 1997. The uranium mining industry of the Bancroft Area: An environmental history and heritage assessment. Trent Univeristy, California,

USA.

Reading, D.G., Croudace, I.W., Warwick, P.E., Britton, R., 2015. A Rapid Dissolution Procedure to Aid Initial Nuclear Forensics Investigations of Chemically Refractory Compounds and Particles Prior to Gamma Spectrometry. Anal. Chim. Acta 900, 1–9.

Robel, M., Kristo, M., Heller, M., 2009. Nuclear forensic inferences using iterative multidimensional statistics, in: Institute of Nuclear Materials Management 50th Annual Meeting,. Tuscon, AZ, USA.

Sima, O., Dovlete, C., 1997. Matrix Effects in the Activity Measurement of Environmental Samples Implementation of Specific Corrections in a Gamma-ray Spectrometry Analysis Program. Appl. Radiat. Isot. 48, 59–69.

Smith, L.I., 2002. A tutorial on Principal Components Analysis.

Švedkauskaitė-LeGore, J., Rasmussen, G., Abousahl, S., Belle, P., 2008. Investigation of the sample characteristics needed for the determination of the origin of uranium-bearing materials. J. Radioanal. Nucl. Chem. 278, 201–209.

Tabachnick, B.G., Fidell, L.S., 2013. Using Multivariate Statistics, 6th ed. Pearson Education Limited, Harlow, UK.

Wallenius, M., Mayer, K., Ray, I., 2006. Nuclear forensic investigations: two case studies. Forensic Sci. Int. 156, 55–62.

Wallenius, W., Mayer, K., Varga, Z., 2014. Procedures and Techniques for Nuclear Forensics Investigations, in: IAEA-TECDOC-1730: Application of Nuclear Forensics in Combating Illicit Trafficking of Nuclear and Other Radioactive Material. IAEA, Vienna, pp. 20–24.

Figure 1

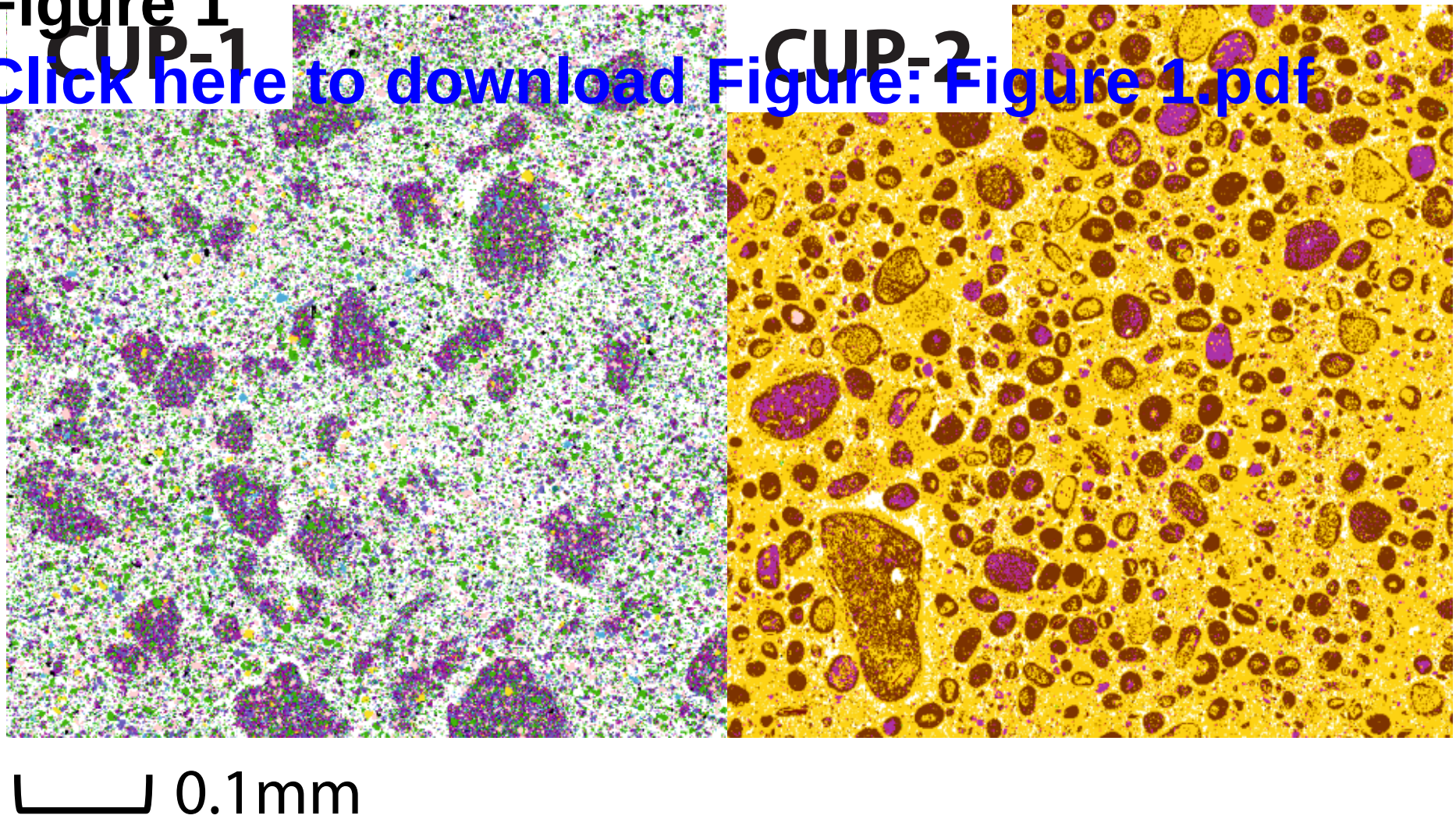

Figure 2

Click here to download Figure: Figure 2.pdf

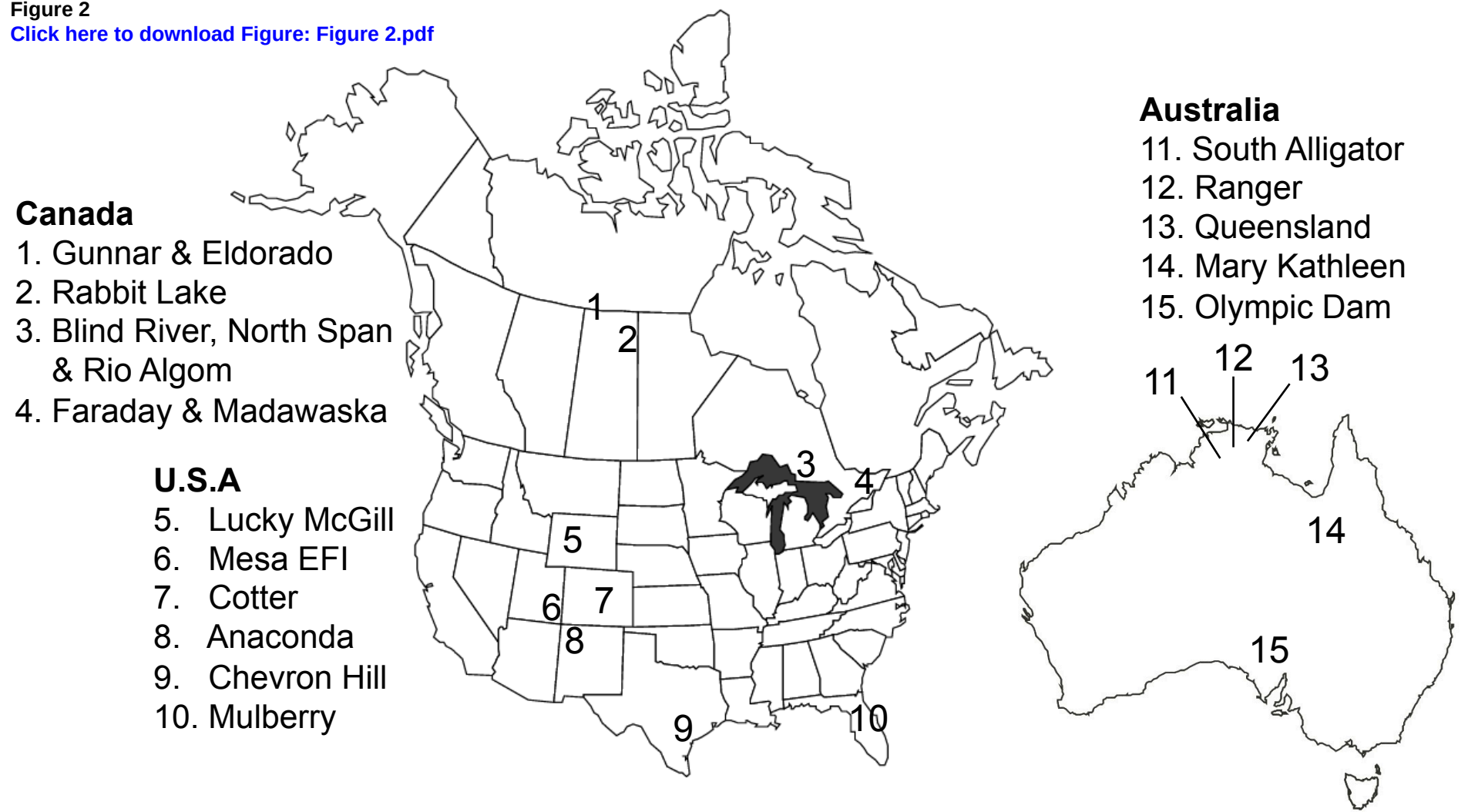

Figure 3 ● Solid Matrix □ Fused Matrix

Click here to download Figure: Figure 3.pdf

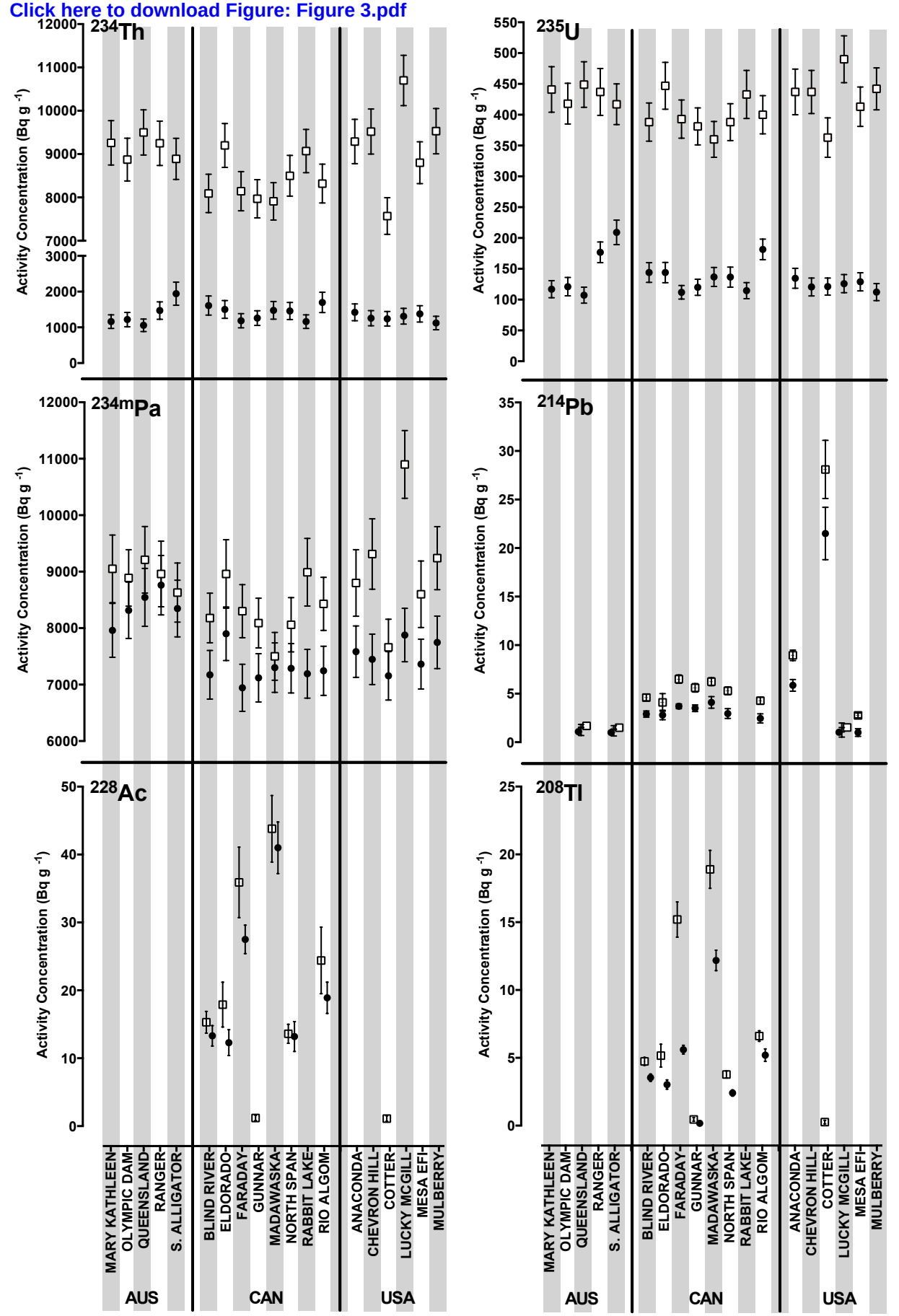

Figure 4

Click here to download Figure: Figure 4.pdf

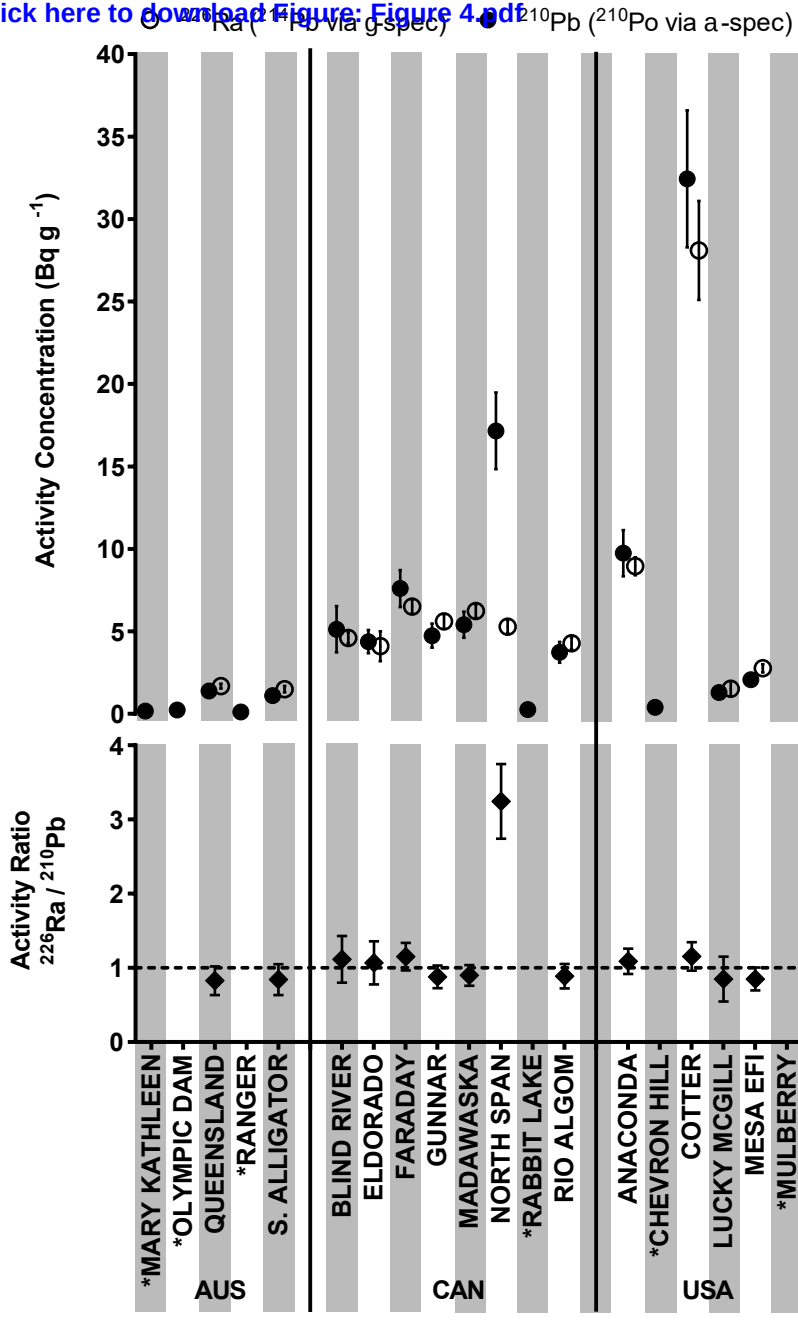

Figure 6

Click here to download Figure: Figure 5.pdf

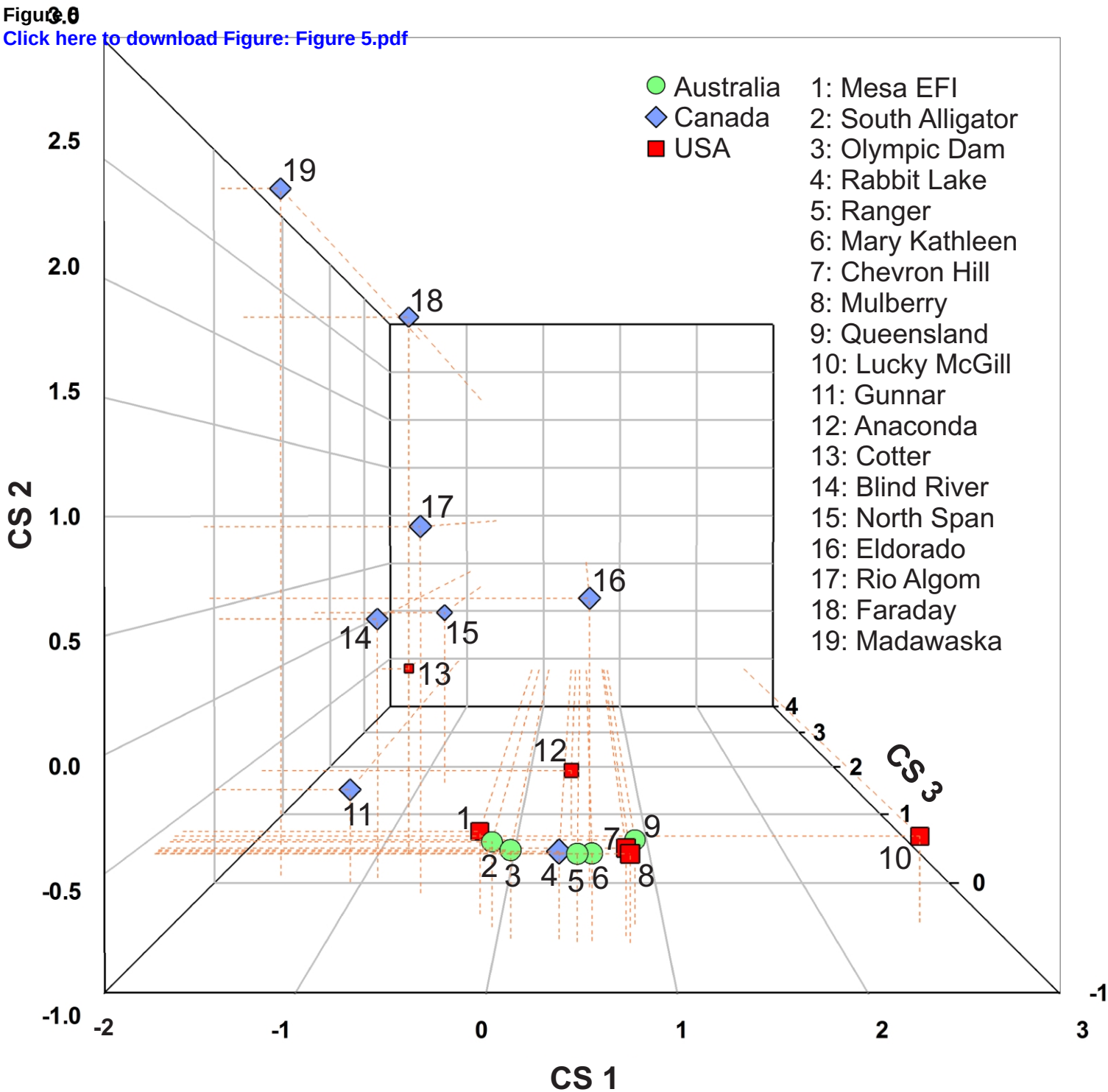

Figure 6

Click here to download Figure: Figure 6.pdf